Adaptive cancellation of self-generated sensory signals in a whisking robot

S. R. Anderson, M. J. Pearson, A. G. Pipe, T. J. Prescott, P. Dean and J. Porrill

***Abstract*—Sensory signals are often caused by one's own active movements. This raises a problem of discriminating between self-generated sensory signals and signals generated by the external world. Such discrimination is of general importance for robotic systems, where operational robustness is dependent on correct interpretation of sensory signals. Here we investigate this problem in the context of a whiskered robot. The whisker sensory signal comprises two components: one due to contact with an object (externally-generated) and another due to active movement of the whisker (self-generated). We propose a solution to this discrimination problem based on adaptive noise cancellation, where the robot learns to predict the sensory consequences of its own movements using an adaptive filter. The filter inputs (copy of motor commands) are transformed by Laguerre functions instead of the often-used tapped-delay line, which reduces model order and therefore computational complexity. Results from a contact detection task demonstrate that false positives are significantly reduced using the proposed scheme.**

***Index Terms*—Learning and Adaptive Systems, Neurorobotics, Force and Tactile Sensing, Noise Cancellation, Laguerre Functions**

I. Introduction

ACTIVE exploration of the environment is a necessary behavioural feature of both animals and mobile robots, for the purposes of navigation, object localization and object recognition. However, active movements will often generate sensations in their own right, leading to a discrimination problem: what sensory signals are caused by one's own movements and what sensory signals are caused by the external world? It is essential that an autonomous agent, either animal or robot, is able to make this distinction in order to interact with the environment in a robust manner. Falsely interpreting sensations could lead to catastrophic consequences for a robot, especially when dealing with threats or opportunities.

Recently, we have encountered an instance of this very problem in the operation of a whisking mobile robot, a prototype of which is described in [1] and [2]. **Robotic whisking, a current area of active research [1], [3]–[7], has potential advantages for exploration when other senses such as vision are compromised, for instance underground, underwater and in smoky environments [8].** When our robot actively whisks against an object, a 'contact' signal is generated due to vibration of the whisker. The contact is sensed by a biomimetic follicle, which records movements of the whisker base. However, actively moving the whisker also generates a sensory signal due to inertial movement of the whisker base in the follicle. Here we regard this 'whisking' signal as self-generated noise because it interferes with the contact signal, which is of primary interest. One simple task that we require the robot to perform is object detection using its whiskers, as a prelude to more complex tasks such as object recognition and building a spatial map. Currently, the sensitivity of object detection in the robot is poor because the threshold level for detecting contacts must be raised relatively high, to prevent activation by the self-generated whisking signal.

Consideration of the problem of discriminating between self- and externally-generated sensations is long established in the biological and neurosciences literature (for a discussion see [9]). As early as the 1950s von Holst coined the term *re-afference principle*[1] to describe self-generated sensations [10]. To solve the re-afference problem, von Holst suggested that a copy of the motor command could be retained in the central nervous system, which would be used to cancel the re-afferent signal [10]. This idea has been refined further over the years, leading to the notion that the brain could learn internal dynamical models that predict the sensory consequences of motor actions, thus leading to an ability to discriminate between self-generated and externally-generated signals [11]–[15]. An associated interpretation of this principle was made in the study of electric fish, where the notion of re-afference was specifically connected to adaptive noise cancellation [16]–[18], which is where an adaptive filter learns to cancel additive noise from a signal of interest [19].

Although the uses of predictive models for robotic control are well-known (e.g. Smith predictor, generalised predictive control and self-tuning regulator), it is only more recently that investigation into their related use in recognising and suppressing self-generated signals has emerged in the field of robotics [20]–[22]. This, we suggest, is likely to be a crucial area of work for improving autonomous robotic behaviour. Here, we propose a generic framework for cancelling self-generated sensations in robotic systems, motivated from the biological suggestions of utilising motor command to predict the sensory consequences of movement. We show that for

S. R. Anderson and T. J. Prescott are with the Active Touch Laboratory, University of Sheffield, Sheffield, UK (email: s.anderson@sheffield.ac.uk; t.j.prescott@sheffield.ac.uk)

M. J. Pearson and A. G. Pipe are with the Bristol Robotics Laboratory, Bristol, UK (email: martin.pearson@brl.ac.uk; tony.pipe@brl.ac.uk).

P. Dean and J. Porrill are with the Centre for Signal Processing in Neuroimaging and Systems Neuroscience, University of Sheffield, Sheffield, UK (email: p.dean@sheffield.ac.uk; j.porrill@sheffield.ac.uk).

[1]In the neurosciences, inputs and outputs to and from the central nervous system are known as afference and efference respectively. Hence, 're-afference' describes sensory signals produced by motor actions of the individual. The term 'ex-afference', on the other hand, describes sensory signals caused by the external environment.

linear systems our proposed scheme corresponds to classic adaptive noise cancellation [19], where the input from the external environment is filtered by a combination of controller and plant dynamics.

For small mobile robotic applications, such as that considered here, it is important to minimise the computational complexity of signal processing algorithms in order to reduce power consumption and maximise energy efficiency. Hence, in this investigation we use linear filter basis functions to implement the adaptive filter in the noise cancellation scheme. This leads to reduced model order compared to the standard tapped-delay line implementation, which is computationally advantageous for embedded applications in autonomous robots. To demonstrate the utility of the scheme we apply the noise cancellation algorithm to the contact detection problem (described above) in our whisking robot. **The noise cancellation algorithm is based on the standard approach described in [19]. The tapped delay line is replaced by linear filters in order to reduce computational complexity, an approach advocated in the system identification literature for reducing model order [23]. We use a bioinspired approach of defining the reference noise as the copy of whisking motor command. This scheme links to the biological perspective on internal models: the robot learns to represent its own movement dynamics. Previously we have presented elements of this work in abstract form, where the self-generated sensations of the robot rat were cancelled using a tapped-delay line adaptive filter [24].**

The paper is organised as follows. The adaptive noise cancellation scheme, adaptive filter structure and algorithm are derived in section II. The results from predicting sensory consequences of movement during free-whisking and enhancing contact detection are presented in section III. The results from the noise cancellation scheme implementation and potential directions of future work are discussed in section IV and the investigation is summarised in section V.

II. Methods

The problem of cancelling noise from a signal can be solved optimally using the Wiener filter [25], the principles of which lead to a fixed filter. However, the design of fixed filters relies on *a priori* knowledge of signal statistics and also assumes that the signal will be stationary. The ability to adapt based on changes in task, environment and robot dynamics (e.g. a broken whisker) is an essential feature of an autonomous robot. Hence, the solution framework we develop here is based on the adaptive filter approach. We first explain the adaptive noise cancellation method and then relate it to self-generated noise and specifically the whisker contact detection problem. We then present a computationally efficient implementation of the adaptive finite impulse response (FIR) filter, using Laguerre functions.

A. Adaptive noise cancellation for self-generated sensory signals

Adaptive noise cancellation makes use of a reference noise u to cancel additive noise v from a signal of interest s where only the combined signal $x = s+v$ is observed [19], see figure 1(a). The key point is that the reference noise is uncorrelated with the signal but is correlated, via a 'noise channel', with the additive signal noise. **An adaptive filter learns the dynamics of the noise channel and produces the output y, which is the noise cancelling signal**. So the noise cancellation scheme output z at sample time t is

$$z_t = x_t - y_t, \tag{1}$$

$$z_t = s_t + v_t - y_t. \tag{2}$$

Assuming that all signals are zero-mean and the reference noise u_t is uncorrelated with s_t, but is correlated with v_t, then by squaring (2) and taking expectations, we obtain an expression for the covariance, or power, in the noise cancellation scheme output,

$$E\left[y_t^2\right] = E\left[s_t^2\right] + E\left[(v_t - y_t)^2\right] \tag{3}$$

Inspection of (3) shows that adjustments in the filter output will not affect the signal power $E\left[s_t^2\right]$. Therefore the power in $E\left[(v_t - y_t)^2\right]$ is minimised when the cancellation scheme output power is minimised,

$$\min E\left[y_t^2\right] = E\left[s_t^2\right] + \min E\left[(v_t - y_t)^2\right] \tag{4}$$

Hence, minimising the total output power of the cancellation scheme is equivalent to minimising the output noise power. Therefore the output of the cancellation scheme may be used as the error signal e_t to drive filter adaptation, i.e. $e_t = z_t$, which minimises the filter prediction error of the noise in a least-squares sense.

In the context of cancelling self-generated noise, we can write down a conceptual model of the self-generated noise cancellation scheme, by analogy with figure 1(a), replacing the reference noise with motor command, shown in figure 1(b). To obtain the cancellation scheme for the specific case of the whisking robot, it is necessary to consider the robot whisker control scheme and relate that to the generic scheme in figure 1(b). The whisker plant is controlled by a PID controller and motor in a negative feedback loop. We model the output of this control loop (whisker angle) as the input to the follicle sensor. We model the contact signal as an additive disturbance to the whisker and is therefore within the feedback loop. Hence, assuming that each component of the system can be represented by a linear filter, the observed whisker sensory signal can be described as the sum of the two input signals, filtered by follicle, whisker plant and controller dynamics,

$$x_t = G(q)u_t + H(q)d_t \tag{5}$$

where q is the shift operator ($qu_t = u_{t+1}$), d_t **is the object contact input signal**,

$$G(q) = \frac{F(q)C(q)P(q)}{1 + C(q)P(q)}, \tag{6}$$

$$H(q) = \frac{F(q)P(q)}{1 + C(q)P(q)}, \tag{7}$$

and $F(q), C(q)$ and $P(q)$ are linear discrete-time filters representing the follicle, controller and plant dynamics respectively.

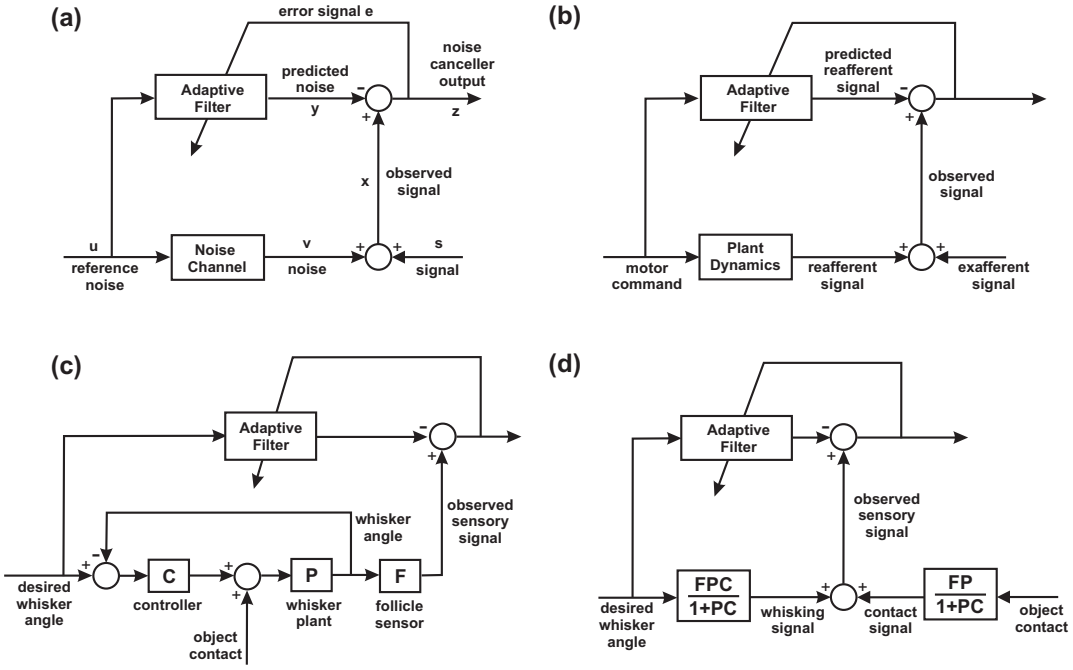

Fig. 1. The link between adaptive noise cancellation, the generic cancellation of self-generated sensory signals (using copy of the motor command) and the specific cancellation of the whisking component from combined whisker/contact sensory signals. (a) Classic adaptive noise cancellation. The reference noise signal is assumed to be known and correlated with the noise but uncorrelated with the signal. (b) A conceptual mapping of the adaptive noise cancellation scheme into the framework of cancelling self-generated sensory signals. This scheme uses motor command in analogy to the reference noise. (c) The robot whisker control and sensory scheme with noise cancelling adaptive filter. The controller, plant and follicle sensor are represented by linear transfer functions C, P and F respectively. (d) The robot whisking scheme reinterpreted in the architecture of classic adaptive noise cancellation.

This scheme is shown in figure 1(d), which is clearly related to the original noise cancellation scheme in 1(a). In the context of the noise cancellation scheme, the contact signal corresponds to $s_t = H(q)d_t$ and the whisking signal corresponds to $v_t = G(q)u_t$, which leads to an analogous expression of (2), for the whisker signal cancellation scheme,

$$z_t = H(q)d_t + G(q)u_t - y_t. \tag{8}$$

The adaptive filter must therefore learn the dynamics of the closed loop expression $G(q)$ using the whisking motor command input u_t, which we assume is uncorrelated with the contact signals $H(q)d_t$.

B. Adaptive FIR filter with LMS learning rule

Typically, an adaptive FIR filter is used to learn the noise channel dynamics of the reference noise to signal noise transformation, where the filter is described as

$$y_t = \sum_{k=1}^{n} w_t^{(k)} u_{t-k+1} \tag{9}$$

where y_t is the filter output at sample time t (prediction of self-generated noise), u_t is the filter input (copy of motor command), the notation u_{t-k} indicates tap delays of the input signal, $w_t^{(k)}$ is the k^{th} time-varying filter weight and n is the filter order. The filter can be written compactly in vector notation as

$$y_t = \mathbf{u}_t \mathbf{w}_t \tag{10}$$

where $\mathbf{u}_t = [u_t, \ldots, u_{t-n+1}]$ and $\mathbf{w}_t = [w_1, \ldots, w_n]^T$.

The parameters of the adaptive FIR filter are adapted here by the least-mean-square (LMS) rule of Widrow and Hoff [26], [27],

$$\mathbf{w}_{t+1} = \mathbf{w}_t + \mu \mathbf{u}_t e_t \tag{11}$$

where μ is a learning rate parameter, e_t is the filter prediction error and the product term $\mathbf{u}_t e_t$ is a sample estimate of the squared filter prediction error gradient vector. The learning rate term μ can be a constant but here we use normalised LMS (NLMS), where $\mu = \beta / ||\mathbf{u}_t||^2$, where β is a constant. The NLMS rule typically increases the rate of convergence [27]. Regarding convergence, subject to the stability of the implementation, the NLMS rule converges to the Wiener filter solution [28].

C. Reducing model order of the FIR filter using Laguerre functions

The FIR filter implemented with a tapped-delay line normally requires a large number of parameters, which is undesirable due to excessive computational complexity. The reason for this is that the true system impulse response often decays slowly with respect to the sample rate, requiring many tapped-delays and associated parameters. One method for reducing the order of the FIR filter is to decompose the description of the impulse response into a weighted sum of linear basis functions [23],

$$y_t = \sum_{k=1}^{p} w_t^{(k)} L_k(q, \boldsymbol{\gamma}) u_t \tag{12}$$

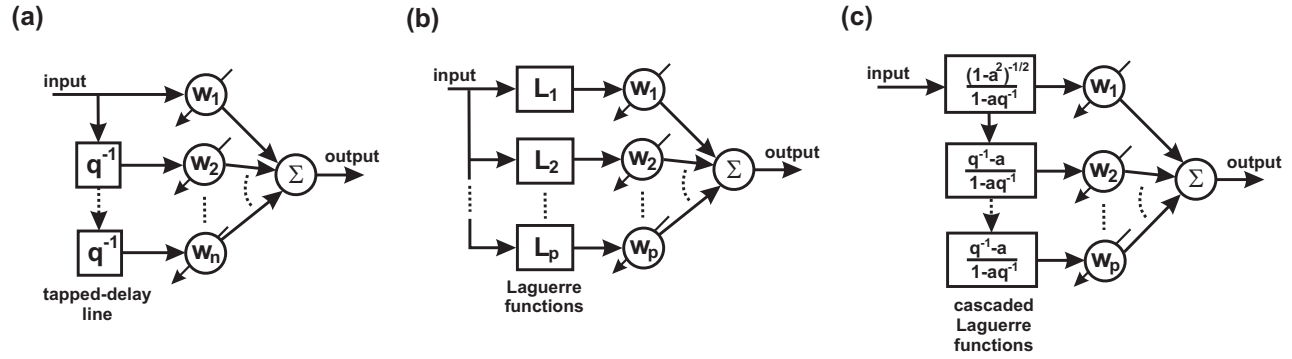

Fig. 2. Various possible structures of the adaptive FIR filter. (a) The standard tapped-delay line implementation of the adaptive FIR filter. (b) The Laguerre function implementation of the adaptive FIR filter. (c) The cascaded Laguerre function implementation of the adaptive FIR filter.

where the number of filter weights is p, $L_k(q,\boldsymbol{\gamma})$ is a basis function that is a linear discrete-time filter and $\boldsymbol{\gamma}$ is the vector of filter parameters. The adaptive filter output can be compactly expressed as

$$y_t = \boldsymbol{\psi}_t \mathbf{w}_t, \tag{13}$$

$$\boldsymbol{\psi}_t = \left[L_1(q,\boldsymbol{\gamma})u_t, \ldots, L_p(q,\boldsymbol{\gamma})u_t\right]. \tag{14}$$

The basis functions replace the tapped-delay line and, importantly, can greatly reduce the number of model parameters, therefore typically $p << n$. The basis functions that we use here have been extensively investigated in the system identification and signal processing literature, namely Laguerre functions (LFs) [29]–[32]. The LFs are attractive for dynamic system descriptions because they form an orthonormal basis for white noise inputs (as do tapped-delay-lines), yet they are insensitive to the choice of sample rate (unlike tapped-delay-lines). The sequence of LFs is defined as

$$L_k(q,\boldsymbol{\gamma}) = \frac{\sqrt{(1-a^2)}}{1-aq^{-1}}\left(\frac{q^{-1}-a}{1-aq^{-1}}\right)^{k-1} \quad \text{for } k = 1,\ldots,p, \tag{15}$$

where q^{-1} is the backward shift operator and the filter parameter vector $\boldsymbol{\gamma}$ is composed of only a single element $\gamma = a$. In principle other basis functions may be used to describe the FIR filter, such as Kautz functions [30] and generalised bases [33]. However, as will be seen in the results section, LFs describe the data accurately and have the advantage of a simple parameterisation (requiring the selection of only one unknown filter parameter a).

The LF parameter a was selected here by use of a separable least-squares algorithm [34]. Separable least-squares is commonly applied to optimisation problems where the variables naturally separate into linear and nonlinear sets, improving convergence rate and numerical conditioning [35]. In the case of LFs, the adaptive filter weights $\mathbf{w}$ comprise the linear set of parameters and the filter parameter a is defined as the (only) nonlinear parameter. The optimal filter weights can be estimated (in a batch mode offline, from N samples) by least-squares for any given value of a,

$$\mathbf{w}_{LS} = \Psi(a)^{\dagger}\mathbf{x} \tag{16}$$

where $\Psi(a) = \left[\boldsymbol{\psi}_1(a)^T, \ldots, \boldsymbol{\psi}_N(a)^T\right]^T$, $\mathbf{x} = [x_1, \ldots, x_N]^T$ and $\dagger$ indicates the pseudo-inverse. In outline, the weights $\mathbf{w}_{LS}$ were estimated by least-squares within each iteration of a nonlinear optimisation of the parameter a, thus avoiding their explicit inclusion in the nonlinear search. The cost function used to optimise the parameter a was the root-mean-squared (RMS) filter prediction error. The Nelder-Mead simplex algorithm was applied to solving the nonlinear optimisation problem (using the Matlab function *fminsearch*).

Regarding the on-line implementation of the LFs in a robotic system, the LFs can be implemented as a cascade of first order filters. In fact the LFs in (15) are naturally defined as the product of first order filters, hence a cascade is simple to implement directly from inspection of (15) in terms of a single parameter a, where the first LF is

$$\Lambda_1(q,\boldsymbol{\gamma}) = \frac{\sqrt{1-a^2}}{1-aq^{-1}}, \tag{17}$$

and the subsequent filters are each defined as

$$\Lambda_2(q,\boldsymbol{\gamma}) = \frac{q^{-1}-a}{1-aq^{-1}}. \tag{18}$$

A cascade of first order filters has two distinct advantages in comparison to separately implementing each LF (the direct-form). Firstly, the number of multiplications is reduced from $2p(p+1)/2$ in the case of separate LFs, to just $2p$ for the cascade-form. Secondly, the cascade-form of an infinite-impulse response filter (such as an LF) typically has improved numerical robustness compared to the direct-form for finite-word-length implementations [36]. Different possible structures of the adaptive filter are compared in figures 2(a)-(c).

D. Adaptive noise cancellation algorithm

The adaptive noise cancellation algorithm, incorporating the cascade of first order LF filters and parameter adaptation by NLMS, is described in Algorithm 1. The algorithm requires the specification of three parameters before implementation on-line, which are (i) the LF filter parameter a, (ii) the number of LFs p and (iii) the learning rate parameter β. Selection of these parameters is task specific and is discussed for the whisking robot application in the Results section.

The computational complexity of Algorithm 1 is $\mathcal{O}(p)$, where p is the number of LF weights, which is typical of

Algorithm 1 Adaptive Self-Generated Noise Cancellation

1: $\psi_t^{(1)} = \Lambda_1(q, \boldsymbol{\gamma})u_t$ {filter input through first LF}
2: **for** $j = 2$ to p **do**
3: $\quad \psi_t^{(j)} = \Lambda_2(q, \boldsymbol{\gamma})\psi_t^{(j-1)}$ {cascade of LFs}
4: **end for**
5: $y_t = \boldsymbol{\psi}_t \mathbf{w}_t$ {adaptive filter output}
6: $z_t = x_t - y_t$ {noise cancellation scheme output}
7: $\mu_t = \frac{\beta}{\boldsymbol{\psi}_t \boldsymbol{\psi}_t^T}$ {learning rate}
8: $\mathbf{w}_{t+1} = \mathbf{w}_t + \mu_t \boldsymbol{\psi}_t z_t$ {parameter adaptation}

	Tapped-Delay-Line	Cascade of Laguerre Functions
Input Filtering	0	3p
Adaptive Filter Output	n	p
Learning Rate	n+1	p+1
Parameter Adaptation	n	p
Total	3n+1	6p+1

TABLE I
COMPUTATIONAL COMPLEXITY (NUMBER OF MULTIPLICATIONS AND DIVISIONS PER ITERATION) FOR ADAPTIVE FILTERING VIA A TAPPED-DELAY-LINE IMPLEMENTATION COMPARED TO A CASCADE OF LAGUERRE FUNCTIONS (ALGORITHM 1).

LMS algorithm implementations [27]. This linearity in computational complexity is an attractive feature of LMS adaptation and is particularly suited to applications in robotics systems where it is important to minimise computational requirements.

The total computational complexity of Algorithm 1 (using a cascade of LFs) is compared to a tapped-delay-line equivalent in table I. We note that although the complexity would be higher for LFs if $p = n$ in fact for a tapped-delay-line and LF filter implementation of similar accuracy typically $p << n$ [30]. Hence, we suggest that use of LFs will often be an attractive option with regard to reducing computational complexity. This point is specifically addressed for the whisking robot application in the Results section.

E. Whisking Robot

The whisking robot utilised in this study is a development of the prototype described in [1] and [2], see figure 3. The new whisking robot, SCRATCHbot [7], has 18 whiskers arranged in 3 columns of 3 whiskers per column on each side of the robot head (i.e. 9 on each side). Each of the columns are independently actuated using DC motors, providing 120 degrees of rotation (figure 4).

The reference trajectory of each column is currently specified by the operator and controlled using a proportional-integral-derivative (PID) position control algorithm implemented in a local micro-controller **(with a sample rate of 200 Hz)**. Each of the plastic whiskers (made from acrylonitrile butadiene styrene - ABS) has a small magnet bonded to the base which, in turn, is mounted into a flexible polymer follicle. Any movement of the magnet is monitored in 2-dimensions using a Hall effect sensor located inside the follicle. Therefore, any deflections of the whisker shaft are represented as displacement vectors at the base.

Taking inspiration from mammalian vibrissal fields, the lengths and thicknesses of the whiskers vary across the array, with the longer thicker whiskers located toward the rear. The results of this study were taken from a 200mm long whisker shaft with a circular cross-section of 2mm diameter at the base, tapering linearly to 0.6mm diameter at the tip.

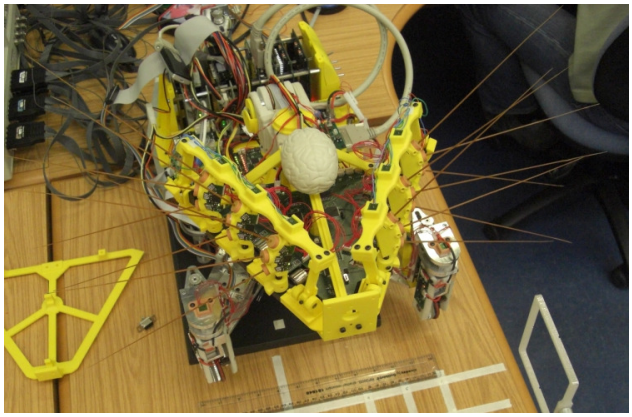

Fig. 3. The whisking robot: SCRATCHbot.

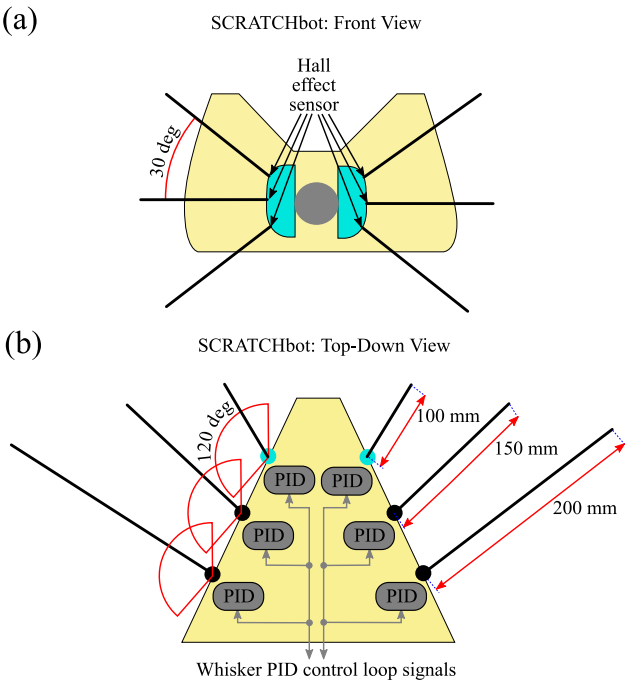

Fig. 4. Diagram of SCRATCHbot head. (a) Front view. The front two columns of whiskers are illustrated. The three rows of whiskers on each side of the head are spread by 30 degrees. The movement of each whisker activates a Hall effect sensor that gives a measure of whisker displacement. (b) Top-down view. All six columns of whiskers are illustrated. Each column of whiskers is independently actuated by a DC motor, under PID control. Each column can move through 120 degrees of rotation. The lengths of the whiskers decrease from front to back of the head (100-200 mm).

F. Experiment Design

A single whisker on the robot (rear column, middle row of the 3×3 array) was driven in two separate experiments, without contacts (free-whisking) and with contacts, where each run was of two minutes in duration. Each data set was collected under head fixed conditions. The free-whisking data was used

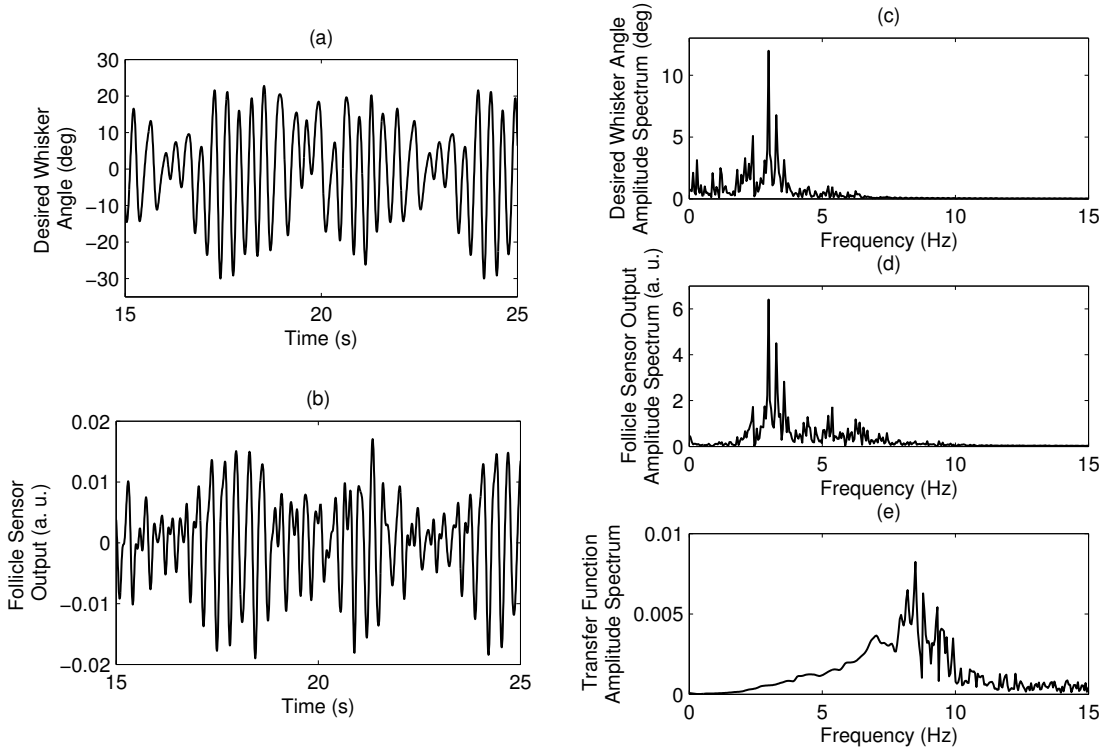

Fig. 5. Robotic whisker input-output signals (desired whisker angle and follicle sensor output respectively). (a) Desired whisker angle signal, zoomed on the time-axis to a typical 10 second segment. The desired whisker angle signal was obtained from real rat whisking recorded by Towal and Hartmann [37]. (b) Follicle sensor output signal, zoomed on the time-axis to a typical 10 second segment. (c) Desired whisker angle amplitude spectrum. (d) Follicle sensor output amplitude spectrum. (e) Robotic whisker transfer function amplitude spectrum, obtained from the empirical transfer function estimate (ETFE).

to design the LFs prior to the contact detection task. In the contact detection experiment, the contact object (a flexible plastic rod, 80mm long, 1.5mm in diameter) was held in the path of the whisker at random times and removed after contact. Contact times of the whisker were obtained with coarse accuracy (to the nearest second) by use of a video recording of the experiment. Precise contact times of the whisker were obtained from applying the noise cancellation algorithm to the data and visually inspecting the resulting 'clean' signal, with reference to the contact times obtained from the video recording. Each input-output data set was processed and analysed offline using Matlab.

We drove the whiskers of the robot with an input signal (desired whisker angle) obtained from real rat whisking recorded by Towal and Hartmann [37]. Two typical free-whisking trials of $\sim$1.5 seconds in duration were concatenated together to form an input signal of $\sim$3 seconds. The original signals had a strong periodic component in the whisking at $\sim$8 Hz. We scaled the whisking signal to reflect the larger size of the robot rat (compared to an actual rat). Therefore we lowered the whisking rate by redefining the sample rate from 250 Hz to 100 Hz, thereby shifting the whisking rate down by a factor of 2.5, so that the strong periodic component of whisking occurred at $\sim$3 Hz. The resulting signal, of duration $\sim$7.5 seconds was looped for 2 minutes to form the input signal used in the free-whisking and contact experiments.

The characteristics of the input-output data from the robot whisker plant (desired whisker angle and follicle sensor output respectively) are shown in figures 5(a)-(d), from free-whisking. The dynamic characteristics of the robot whisker plant, equivalent to the transfer function $G(q)$ defined in (6), are described in figure 5(e) by the empirical transfer function estimate (ETFE) [23]. The ETFE is the ratio between the Fourier transforms of the output and input and was obtained in this case by the Matlab function *tfestimate*, which uses Welch's method to obtain the estimate [23]. The input-output signals were sampled from the robot at 200 Hz and low-pass filtered at 5 Hz to attenuate nonlinear harmonics in the output signal. Although in principle it would be possible to describe these nonlinearities with a nonlinear FIR filter, that was outside the scope of this investigation and did not affect the main result of enhancing contact detection.

III. Results

This section presents results for the adaptive filter design and application to the task of enhancing whisker contacts in the presence of self-generated noise. The task was to dynamically model the whisker plant (desired whisker angle-to-follicle sensor output transformation) and use this model to cancel the self-generated sensory signal using an adaptive FIR filter (Algorithm 1). The results are divided into three sections: LF selection, prediction of sensory consequences of movement and contact detection.

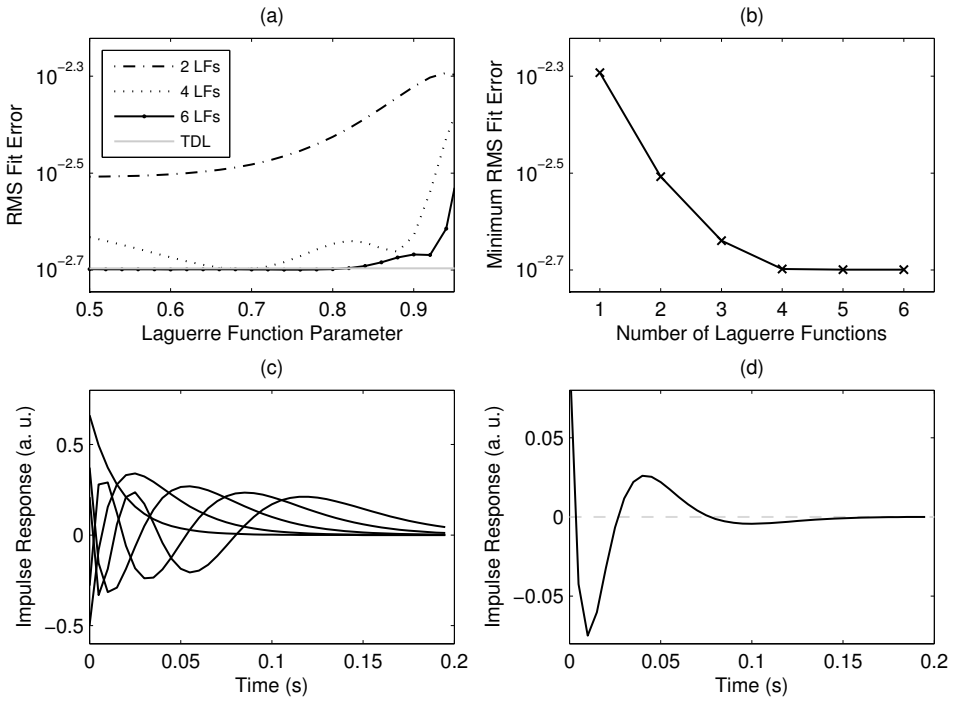

Fig. 6. Structure detection for the Laguerre functions. (a) Comparison of FIR filters composed of 2 to 6 Laguerre functions (LFs) in terms of root-mean-square (RMS) fit error along with the fit error of a tapped-delay line (TDL) FIR filter (40 taps), where the Laguerre function parameter a was varied systematically between 0.5 and 0.96. (b) Comparison of Laguerre function FIR filters in terms of minimum RMS fit error. (c) Impulse responses of the Laguerre basis functions 1 to 5, which are weighted and summed to form the whisker plant impulse response (where $a = 0.75$). (d) Whisker plant impulse response described by the Laguerre function filter (5 LFs), obtained from the separable least-squares fit to the free-whisking data (where $a = 0.75$).

A. Laguerre function structure detection

The LF structure detection task was composed of selecting two parameters: the filter parameter a and the number of LFs p. The number of LFs p was selected first by comparing the FIR filter prediction of the follicle sensor output signal for different numbers of LFs. The optimal fit of each LF filter was obtained in a batch mode using least-squares. We fitted 1 to 6 LFs (using the free-whisking data), with the filter parameter a systematically varied from 0.5 to 0.96. The root-mean-square (RMS) fit error was compared across the different numbers of basis functions and selected results are shown in figure 6(a). We found that at least 4 LFs were required to model the dynamics of the whisker plant, based on inspection of the knee-point in figure 6(b). Although the accuracy of 4 LFs was similar to 5 LFs we found that the fit error was more sensitive to the choice of a when using 4 LFs. Hence, we selected $p = 5$.

After selecting the number of LFs the parameter a was estimated using a separable least-squares algorithm as described in the Methods (where the choice of the single parameter a defined the dynamics of all LFs). The optimal parameter estimate was $a = 0.75$. The impulse responses of the 5 selected LFs with optimal parameter estimate $a = 0.75$ are shown in figure 6(c). The impulse response of the whisker plant (identified by the separable least-squares algorithm) is plotted in figure 6(d), which shows that the response is mildly oscillatory and decays after 200 ms.

Only 5 LFs were required here to model the whisker plant dynamics. A comparable filter length implemented by a tapped-delay line would require 40 taps. Hence, the LF implementation resulted in a significant reduction in model order, with a corresponding reduction in computational complexity. For this case, the computational complexity of the LF implementation was just 31 multiplications and divisions compared to 121 for the tapped-delay-line (calculated from the totals in Table I). This reduction in number of operations of 74% scales with the number of whiskers (due to the fact that each whisker requires a separate instance of the cancellation algorithm). To illustrate the benefit of using the LFs, recalling that SCRATCHbot has 18 whiskers in total, in the time it would take to process just 4 whiskers using a tapped-delay-line it would be possible to process all 18 whiskers using the LF implementation of Algorithm 1.

B. Prediction of sensory consequences of movement

The adaptive filter was required to learn the whisker plant dynamics on-line (as opposed to the off-line identification used to select the LFs, discussed above). For the case of free-whisking (i.e. no contacts) the adaptive filter output y_t should closely match the output of the follicle sensor x_t. Therefore after defining the LFs we ran the adaptive noise cancellation algorithm (Algorithm 1) on the free-whisking data to confirm that the adaptive filter could accurately learn the whisker plant dynamics. The user-defined parameters in Algorithm 1 were set to $a = 0.75$, $p = 5$ and $\beta = 0.01$. The adaptive filter weights were initialised to zero.

We found that after filter convergence on the free-whisking data the prediction accuracy of the self-generated noise was high. Figure 7(a) and (b) compares the filter output y_t with the follicle output x_t, at the beginning and end of learning respectively. The variance accounted for[2] (VAF) obtained from the final 20 seconds of free-whisking data was VAF=0.94.

C. Contact detection

Apart from the choice of LF function parameter a and the number of LFs p, the only other user-defined parameter necessary to implement Algorithm 1 was the learning rate constant β. **We investigated choice of learning rate parameter with respect to performance in the contact detection task. The metric used to measure performance was signal-to-noise ratio (SNR). The signal power in the SNR measure P_s was defined as the variance of the signal segment 200 ms before and after a contact. The noise power in the SNR measure P_n was defined as the variance of the remainder of the signal after removing the contact segments. Hence, SNR was defined as $SNR = 10\log_{10}(P_s/P_n)$. The SNR measure was obtained after applying Algorithm 1 to the contact data, varying the learning rate between 10^{-4} and 10^{-1}. The optimal learning rate parameter, that maximised SNR, was found to be $\beta \approx 0.004$ (figure 8). The limiting factor on faster learning (i.e. for $\beta > 0.004$) appeared to be due to contacts disrupting adaptation. However, stability was guaranteed even in the presence of these contacts because the filter input was stationary and uncorrelated with object contacts [27].**

After selecting the learning parameter β, we ran Algorithm 1 on the contact data (described in section II-F) to assess the utility of the noise cancellation scheme. **The contact detection experiment was of duration 2 minutes, corresponding to $N = 24,000$ samples at the sample rate of 200 Hz. Parameter adaptation took place at each sample time. Separate analysis on contact-free data showed that at this learning rate prediction accuracy was over 90% within 2 seconds of adaptation.** Contacts in the whisking signal were well amplified (compared to the raw sensory signal) as errors in prediction, shown in figures 9(a) and (b). It is apparent from a visual inspection of figure 9(a) that many of the contacts are effectively hidden within the self-generated noise. By comparison, a visual inspection of figure 9(b) emphasises the utility of the noise cancellation scheme by revealing the location of contacts in the adaptive noise canceller output.

The purpose of the noise cancellation scheme was to enhance contact detection in comparison to using the raw follicle output signal. The method we used for detecting contacts was to apply a threshold to both the follicle output and noise cancellation scheme output. Signal values that exceeded the threshold were classified as contacts. In order to assess the improvement in detecting contacts by the noise cancellation scheme, we used a measure known as the receiver operating characteristic (ROC) curve, which is widely used in classification problems [38]. The ROC curve plots the false positive rate against the true positive rate (where the false and true positive rates are the normalised number of true positives and false positives respectively). We defined the maximum possible number of false positives as the number of forward whisks (due to the fact that each whisk could have potentially signalled a contact). We obtained the ROC curve by systematically varying the contact detection threshold from 0 to 1.1, applying each threshold to the absolute values of the normalised follicle output and cancellation scheme output (i.e. the signals shown in figure 9), and counting the number of resulting true and false positives corresponding to each signal. The ROC curve showed that for the raw signal (follicle sensor output) a true positive rate of 0.95 could only be obtained at the expense of a false positive rate of ∼0.53 (figure 10), which is poor performance. By contrast the clean signal (noise cancellation scheme output) gave a true positive rate of 0.95 for a false positive rate of only ∼0.04 (figure 10). Hence, the use of the cancellation scheme greatly enhanced contact detection for this data set.

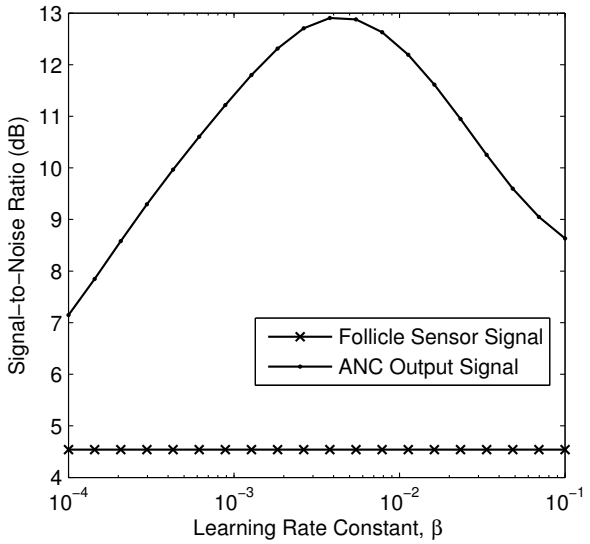

Fig. 8. Variation in signal-to-noise ratio for different rates of learning in the adaptive noise cancellation (ANC) scheme, with baseline comparison to the signal-to-noise ratio obtained from the follicle sensor output. Results were obtained from one presentation of the contact data to the noise cancellation algorithm.

IV. Discussion

A. Improved contact detection by adaptive noise cancellation

We found that the noise cancellation scheme based on the biological principle of using copy of the motor command worked as expected from the theory. The adaptive filter successfully learnt a model of the robot whisker controller-plant dynamics (demonstrated by the adaptive filter learning to predict the sensory consequences of movement during free-whisking). We showed that the particular adaptive FIR filter implementation we chose (cascaded LFs) reduced computational complexity in comparison to a tapped-delay line.

[2]The variance accounted for metric (VAF) is a measure of model fit quality, where VAF=1-var(e)/var(y), where e is the fit error and y is the target data. Hence, a VAF≈1 implies that the model fit is good because the normalised error variance is close to zero. The VAF is also known as the coefficient of determination or r-squared value.

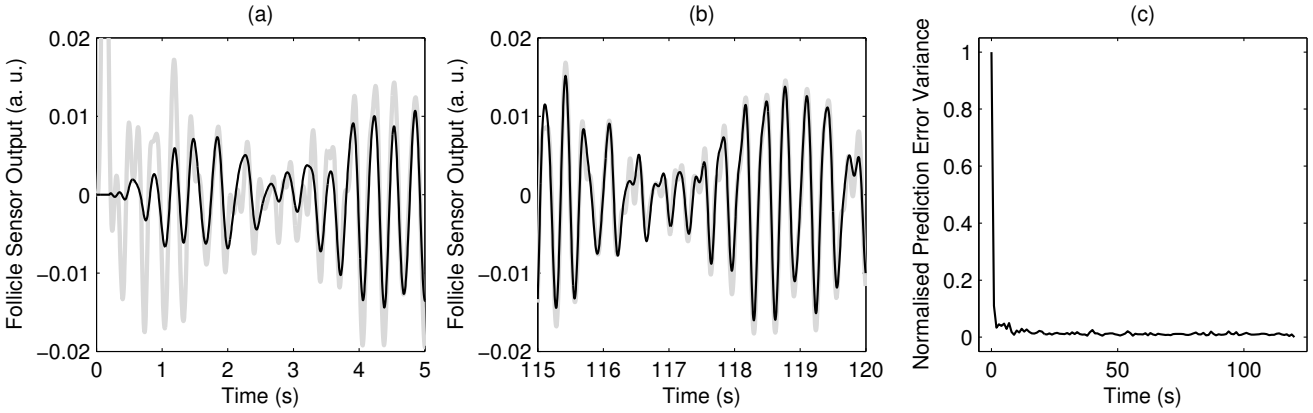

Fig. 7. Prediction of the sensory consequences of active whisking, where the adaptive filter learns over time to predict the whisker follicle sensor output. (a) Start of learning (first 5 seconds). (b) End of learning (final 5 seconds). (c) Normalised variance of the adaptive filter prediction error (where each sample of the variance is taken over 1 second).

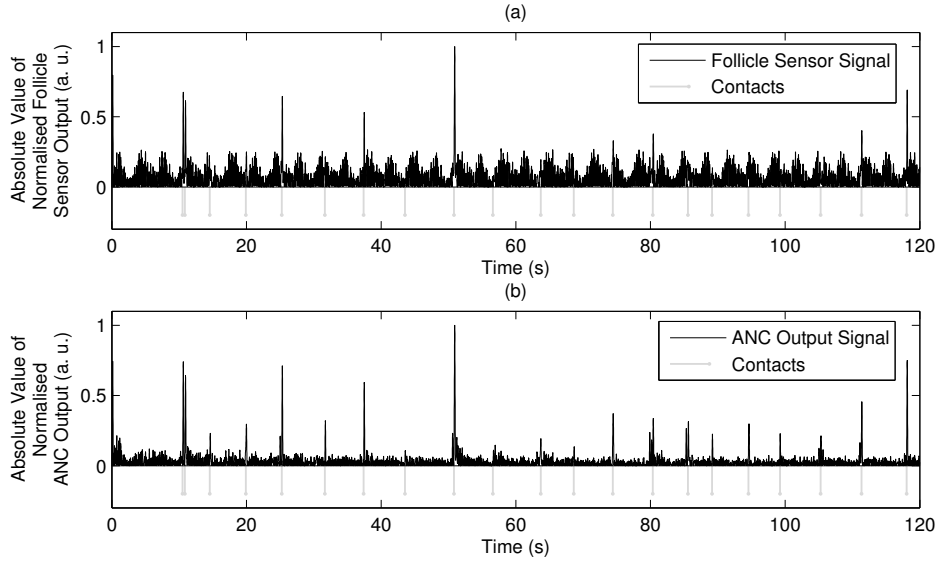

Fig. 9. Adaptive noise cancellation (ANC) scheme applied to the problem of contact detection from the robot whisker sensory signal. (a) The absolute value of the whisker follicle sensor output, normalised by the peak signal value. (b) The absolute value of the adaptive noise cancellation scheme output, normalised by the peak signal value.

We tested the algorithm on contact detection during active robot whisking, where we showed that the use of the noise cancellation scheme led to a much improved ratio of true positives to false positives in comparison to using the raw sensory signal.

Hence, the algorithm (Algorithm 1) that we have developed here is well suited to applications in autonomous robotics because (i) it should lead to improved discrimination between self-generated and externally-generated signals in general robotic tasks (i.e. not limited to whisking), (ii) the implementation is adaptive, hence suitable for on-line learning and (iii) the algorithm is relatively computationally inexpensive (linear in the model order, where order will typically be small due to the use of LFs). **As in the case of generic LMS adaptation schemes, the instance of the noise cancellation algorithm presented here is stable and convergent provided the learning rate is within acceptable bounds, and in addition is also able to track slowly time-varying systems [28].**

B. Computationally efficient algorithm for mobile robotic platforms

The SCRATCHbot platform, like all autonomous mobile robotic platforms, has a limited onboard power supply. A considerable amount of this power is required by the actuators and processors distributed across the platform to control each degree of freedom as well as the Single Board Computer (SBC) and FPGAs used for signal processing, higher level planning and control. Consequently, the chosen SBC represents a compromise between power consumption and computational performance. To overcome the computational constraints of the platform, external processors could be employed and integrated using wireless communication. However, the data

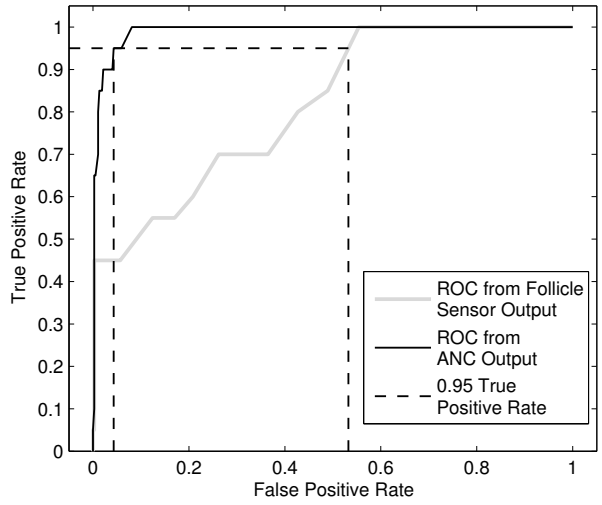

Fig. 10. Receiver operating characteristic (ROC) curve that describes false positive vs. true positive rates of contacts detected at varying threshold levels from (i) the raw follicle sensor output signal and (ii) the clean signal generated by the adaptive noise cancellation scheme.

bandwidths and latencies of conventional wireless protocols do not currently satisfy the requirement for the proposed noise cancellation scheme. Computational efficiency of onboard signal processing algorithms is therefore of utmost importance. Here we have developed a noise cancellation algorithm that focused on reduction of computational complexity by the use of LFs, rather than the commonly used tapped-delay line. The number of computations in this case was reduced by 74% (from 121 to 31 for one whisker output), a highly beneficial improvement for onboard processing.

C. Possible neural substrates of a contact detection scheme in the rat

Given the success of the cancellation scheme considered here, based on adaptive filtering, it is natural to ask whether there exists a comparable functional system in whisking animals such as the rat. It has been reported that rat free-whisking (i.e. with no contacts) generates a sensory signal [39], [40]. This signal is analogous to the self-generated signal observed in our whisking robot. Therefore it is possible that a similar problem of discrimination between self- and externally-generated signals exists in the rat.

In a parallel theme of work we are currently investigating the possibility that the cerebellum is involved in a biological cancellation scheme, where the cerebellum is the structure that performs the role of the adaptive filter [24], [41]. The cerebellum is a natural candidate for this role because of the resemblance of the cerebellar microcircuit to the adaptive filter [42], [43]. The cerebellum has also been particularly associated with the concept of learning internal dynamical models [11], [12], [44].

The adaptive filter is a widely used model of cerebellar processing and the nature of the basis functions used in biological systems is an area of active research. Marr and Albus originally proposed that the granule cell layer implemented a basis that performed a massive expansion recoding of cerebellar (mossy fibre) inputs [45], [46]. An important question is whether the Marr-Albus hypothesis of granule cell layer function is consistent with recent electrophysiological evidence thought to suggest a modest role for granular layer transformation (references in [47]). If this proves to be the case then bases such as the LFs used here, which are much more efficient (and also more biologically plausible) than tapped delay lines, may have applications to biological systems.

V. Summary

This investigation has addressed the problem of cancelling self-generated robotic sensory signals in a generic framework. The choice of reference noise as input to the adaptive filter in the cancellation scheme was motivated by the biological observation that one may use copy of motor commands to predict sensory consequences of movement. The algorithm was based on adaptive FIR filtering, where the filter input was first transformed by LFs (rather than tapped-delay lines) to reduce the filter order and in turn the computational complexity. The cancellation scheme was applied to self-generated sensory signals in a whisking robot. We showed that the cancellation scheme greatly enhanced contact detection on signals recorded from robot whisker contacts, dramatically reducing the false positive rate.

VI. Acknowledgements

The authors would like to thank B. Towal and M. Hartmann for the rat whisking data that was used to generate the input signal to drive the robot whisker. This work was supported by European Union Grant 'Integrating Cognition, Emotion, and Autonomy' (ICEA, IST-027819) and European Union Grant 'Biomimetic Technology for Vibrissal Active Touch' (BIOTACT, ICT-215910).

References

[1] M. J. Pearson, A. G. Pipe, C. Melhuish, B. Mitchinson, and T. J. Prescott, "Whiskerbot: A robotic active touch system modeled on the rat whisker sensory system," *Adaptive Behaviour*, vol. 15, no. 3, 2007.

[2] C. W. Fox, B. Mitchinson, M. J. Pearson, A. G. Pipe, and T. J. Prescott, "Contact type dependency of texture classification in a whiskered mobile robot," *Autonomous Robots*, vol. 26, no. 4, pp. 223–239, 2009.

[3] M. J. Hartmann, "Active sensing capabilities of the rat whisker system," *Autonomous Robots*, vol. 11, no. 3, pp. 249–254, 2001.

[4] D. Kim and R. Moller, "Biomimetic whiskers for shape recognition," *Robotics and Autonomous Systems*, vol. 55, no. 3, pp. 229–243, 2007.

[5] G. R. Scholz and C. D. Rahn, "Profile sensing with an actuated whisker," *IEEE Transactions on Robotics and Automation*, vol. 20, no. 1, pp. 124–127, 2004.

[6] J. H. Solomon and M. J. Z. Hartmann, "Artificial whiskers suitable for array implementation: accounting for lateral slip and surface friction," *IEEE Transactions on Robotics*, vol. 24, no. 5, pp. 1157–1167, 2008.

[7] T. J. Prescott, M. J. Pearson, B. Mitchinson, J. C. W. Sullivan, and A. G. Pipe, "Whisking with robots," *IEEE Robotics and Automation Magazine*, vol. 16, no. 3, pp. 42–50, 2009.

[8] M. J. Hartmann and J. H. Solomon, "Robotic whiskers used to sense features," *Nature*, vol. 443, pp. 525–525, 2006.

[9] K. E. Cullen, "Sensory signals during active versus passive movement," *Curr Opin Neurobiol*, vol. 14, no. 6, pp. 698–706, 2004.

[10] E. von Holst, "Relations between the central nervous system and the peripheral organs," *The British Journal of Animal Behaviour*, vol. 2, no. 3, pp. 89–94, 1954.

[11] S. J. Blakemore, S. J. Goodbody, and D. M. Wolpert, "Predicting the consequences of our own actions: The role of sensorimotor context estimation," *Journal of Neuroscience*, vol. 18, no. 18, pp. 7511–7518, 1998.

[12] S.-J. Blakemore, D. Wolpert, and C. Frith, "Central cancellation of self-produced tickle sensation," *Nature Neuroscience*, vol. 1, no. 7, pp. 635–640, 1998.

[13] M. I. Jordan and D. E. Rumelhart, "Forward models: supervised learning with a distal teacher," *Cognitive Science*, vol. 16, pp. 307–354, 1992.

[14] R. C. Miall and D. M. Wolpert, "Forward models for physiological motor control," *Neural Networks*, vol. 9, pp. 1265–1279, 1996.

[15] D. M. Wolpert, Z. Ghahramani, and M. I. Jordan, "An internal model for sensorimotor integration," *Science*, vol. 269, no. 5232, pp. 1880–2, 1995.

[16] C. C. Bell, J. C. Montgomery, D. Bodznick, and J. Bastian, "The generation and subtraction of sensory expectations within cerebellum-like structures," *Brain Behaviour Evolution*, vol. 50, pp. 17–31, 1997.

[17] J. C. Montgomery and D. Bodznick, "An adaptive filter that cancels self-induced noise in the electrosensory and lateral line mechanosensory systems of fish," *Neuroscience Letters*, vol. 174, pp. 145–148, 1994.

[18] N. B. Sawtell and A. Williams, "Transformations of electrosensory encoding associated with an adaptive filter," *Journal of Neurosience*, vol. 28, pp. 1598–1612, 2008.

[19] B. Widrow, J. R. Glover, J. M. McCool, J. Kaunitz, C. S. Williams, R. H. Hearn, J. R. Zeidler, E. Dong, and R. C. Goodlin, "Adaptive noise cancelling: principles and applications," *Proceedings of the IEEE*, vol. 63, no. 12, pp. 1692–1716, 1975.

[20] K. Gold and B. Scassellati, "Using probabilistic reasoning over time to self-recognize," *Robotics and Autonomous Systems*, vol. 57, no. 4, pp. 384–392, 2009.

[21] P. Manoonpong and F. Worgotter, "Efference copies in neural control of dynamic biped walking," *Robotics and Autonomous Systems*, no. 11, pp. 1140–1153, 2009.

[22] T. Mizumoto, R. Takeda, K. Yoshii, K. Komatani, T. Ogata, and H. G. Okuno, "A robot listens to music and counts its beats aloud by separating music from counting voice," in *IEEE/RSJ International Conference on Intelligent Robots and Systems*, Nice, France, 2008, pp. 1538–1543.

[23] L. Ljung, *System Identification - Theory for the User*, 2nd ed. Upper Saddle River, NJ: Prentice Hall, 1999.

[24] S. R. Anderson, J. Porrill, M. J. Pearson, A. G. Pipe, T. J. Prescott, and P. Dean, "Cerebellar-inspired forward model of whisking enhances contact detection by vibrissae of robot rat," in *Society for Neuroscience Abstracts*, no. 77.2, Chicago, IL, 2009.

[25] N. Wiener, *Extrapolation, Interpolation, and Smoothing of Stationary Time Series*. New York: John Wiley and Sons, 1949.

[26] B. Widrow and M. Hoff, "Adaptive switching circuits," in *IRE WESCON Convention Record*, vol. pt. 4, New York, 1960, pp. 96–104.

[27] B. Widrow and S. D. Stearns, *Adaptive Signal Processing*. New Jersey: Englewood Cliffs, 1985.

[28] D. T. M. Slock, "On the convergence behaviour of the LMS and normalised LMS algorithms," *IEEE Transactions on Signal Processing*, vol. 41, pp. 2811–2825, 1993.

[29] R. E. King and P. N. Paraskevopoulos, "Parametric identification of discrete-time SISO systems," *International Journal of Control*, vol. 30, no. 6, pp. 1023–1029, 1979.

[30] B. Wahlberg, "System identification using Laguerre models," *IEEE Transactions on Automatic Control*, vol. 36, no. 5, pp. 551–562, 1991.

[31] G. W. Davidson and D. D. Falconer, "Reduced complexity echo cancellation using orthonormal functions," *IEEE Transactions on Circuits and Systems*, vol. 38, no. 1, pp. 20–28, 1991.

[32] G. Mandyam and N. Ahmed, "The discrete Laguerre transform: derivation and applications," *IEEE Transactions on Signal Processing*, vol. 44, no. 12, pp. 2925–2930, 1996.

[33] P. S. C. Heuberger, P. M. J. Van den Hof, and O. H. Bosgra, "A generalized orthonormal basis for linear dynamical systems," *IEEE Transactions on Automatic Control*, vol. 40, pp. 451–465, 1995.

[34] L. S. H. Ngia, "Separable nonlinear least-squares methods for efficient off-line and on-line modeling of systems using Kautz and Laguerre filters," *IEEE Transactions on Circuits and Systems II*, vol. 48, no. 6, pp. 562–579, 2001.

[35] G. H. Golub and V. Pereyra, "The differentiation of pseudo-inverses and non-linear least squares problems whose variables separate," *SIAM Journal On Numerical Analysis*, vol. 10, no. 2, pp. 413–432, 1973.

[36] J. G. Proakis and D. G. Manolakis, *Digital Signal Processing*, 3rd ed. New Jersey: Prentice-Hall, 1996.

[37] R. B. Towal and M. J. Hartmann, "Right-left asymmetries in the whisking behavior of rats anticipate head movements," *Journal of Neuroscience*, vol. 26, no. 34, pp. 8838–8846, 2006.

[38] T. Fawcett, "An introduction to ROC analysis," *Pattern Recognition Letters*, vol. 27, pp. 861–874, 2006.

[39] M. Szwed, K. Bagdasarian, and E. Ahissar, "Encoding of vibrissal active touch," *Neuron*, vol. 40, no. 3, pp. 621–630, 2003.

[40] S. C. Leiser and K. A. Moxon, "Responses of trigeminal ganglion neurons during natural whisking behaviours in the awake rat," *Neuron*, vol. 53, pp. 117–133, 2007.

[41] S. R. Anderson, M. J. Pearson, J. Porrill, T. Pipe, T. Prescott, and P. Dean, "Does the cerebellum cancel self-induced noise in whisker sensory signals?" in *Barrels XXI Abstracts*, Baltimore, MD, 2008, pp. 26–27.

[42] M. Fujita, "Adaptive filter model of the cerebellum," *Biological Cybernetics*, vol. 45, pp. 195–206, 1982.

[43] P. Dean and J. Porrill, "Adaptive filter models of the cerebellum: computational analysis," *Cerebellum*, vol. 7, pp. 567–571, 2008.

[44] R. C. Miall, L. O. D. Christensen, O. Cain, and J. Stanley, "Disruption of state estimation in the human lateral cerebellum," *PLOS Biology*, vol. 5, no. 11, pp. 2733–2744, 2007.

[45] D. Marr, "A theory of cerebellar cortex," *Journal of Physiology (London)*, vol. 202, p. 437470, 1969.

[46] J. S. Albus, "A theory of cerebellar function," *Mathematical Biosciences*, vol. 10, pp. 25–61, 1971.

[47] P. Dean, J. Porrill, C.-F. Ekerot, and H. Jorntell, "The cerebellar microcircuit as an adaptive filter: experimental and computational evidence," *Nature Reviews Neuroscience*, vol. 11, pp. 30–43, 2010.